Comparison between transmittance and reflectance measurements in glucose determination using near infrared spectroscopy

Kye Jin Jeon
In Duk Hwang
Samsung Advanced Institute of Technology
Suwon, South Korea

Sangjoon Hahn
Korea Research Institute of Science and Technology
Institute for Gifted Students
Daejeon, South Korea

Gilwon Yoon
Department of Electronics & Information
Seoul National University of Technology
172 Kongneung-dong Nowon-gu
Seoul, South Korea 139-743
E-mail: gyoon@snut.ac.kr

Abstract. Glucose determination based on near-IR spectroscopy is investigated for reflectance and transmittance measurement. A wavelength range is 1100 to 2500 nm, which includes both the combination and overtone bands of glucose absorption. Intralipid solutions are used as samples, where glucose concentrations vary between 0 and 1000 mg/dl. Sample thickness for reflectance is 10 cm and 1- and 2-mm-thick samples are used for transmission. Partial least-squares regression (PLSR) analyses are performed to predict glucose concentrations. The standard errors of calibration are comparable between reflectance and 2-mm-thick transmittance. The reflectance method is inferior to the transmittance method in terms of the standard errors of prediction. Loading vector analysis for reflectance does not show glucose absorption features. Reflected light may not have enough information of glucose since a major portion of detected light has a short optical path length. In addition, prediction becomes more dependent on medium scattering rather than glucose, compared with transmission measurement. Loading vectors obtained from a PLSR transmittance analysis have glucose absorption profiles. The 1-mm-thick samples give better results than the 2-mm-thick samples for both calibration and prediction models. The transmittance setup is recommended for noninvasive glucose monitoring. © 2006 Society of Photo-Optical Instrumentation Engineers. [DOI: 10.1117/1.2165572]

1 Introduction

Diabetic patients are recommended to check their glucose level several times a day, but drawing blood from a finger is painful and there is potential contamination. Ease of use and reduction of pain can encourage more frequent tests and it becomes easier to control glucose level tightly. Near-infrared (NIR) spectroscopy is considered as a promising noninvasive glucose detection method since the NIR region contains the overtone and combination bands of glucose absorption.

Unfortunately, glucose specificity is very low. The specificity is how well glucose is detected without detecting closely related substances. NIR peaks are broad, unlike the fundamental bands, and are overlapped with other blood components. In addition, the normal concentration of blood glucose is too low (74 to 110 mg/dl) compared with other blood components such as hemoglobin (13 to 18 g/dl), protein (6.4 to 8.3 g/dl), total cholesterol (130 to 240 mg/dl), and others. Water, fat, skin, and muscle account for major absorption in biological tissue. In the IR, water is the most dominant absorber and measured spectra are dominated by the water spectrum. Glucose is responsible for less than 0.1% of NIR absorption. In addition, NIR spectra depend on not only glucose absorption but also light scattering properties of tissue. Water-soluble compounds, different cell sizes, and internal inhomogeneous structures influence scattering properties. The scattering property of a sample is determined by the concentration of scatterers and by the difference of the refractive indices between scatterers and medium.

Multivariate statistical analysis such as the partial least squares regression (PLSR) has been used as an effective tool for computing glucose concentration from measured spectra.[1] Preprocessing of measured spectra and the selection of wavelength regions were reported to also be important issues.[2,3] Biological tissue is dominated by light scattering, which further complicates the problem. Not only glucose absorption but also scattering due to glucose molecules changes measured spectra. It has been reported that spectral changes caused by

Address all correspondence to Gilwon Yoon, Electronics & Information, Seoul National University of Technology, 172 Kongneung-dong Nowon-gu, Seoul 139-743, Republic of Korea. Tel: 82–2–970–6419. Fax: 82–2–979–7903. E-mail: gyoon@snut.ac.kr
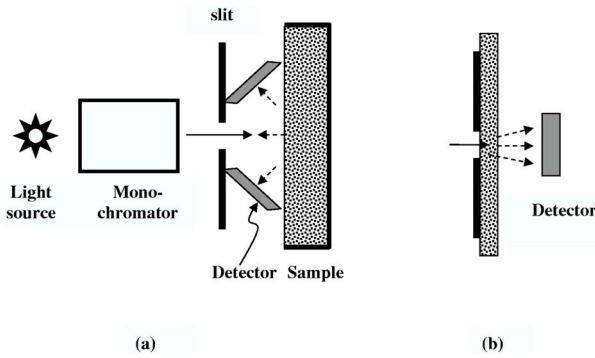
Fig. 1 Schematics for diffuse (a) reflectance and (b) transmittance measurement.

glucose are larger than those caused by absorption.[4] It was proposed that a proper distance between the light source and detector could minimize the effect of medium scattering.[5] One must think about which part of the body is used as a spot for

(a)

(b)
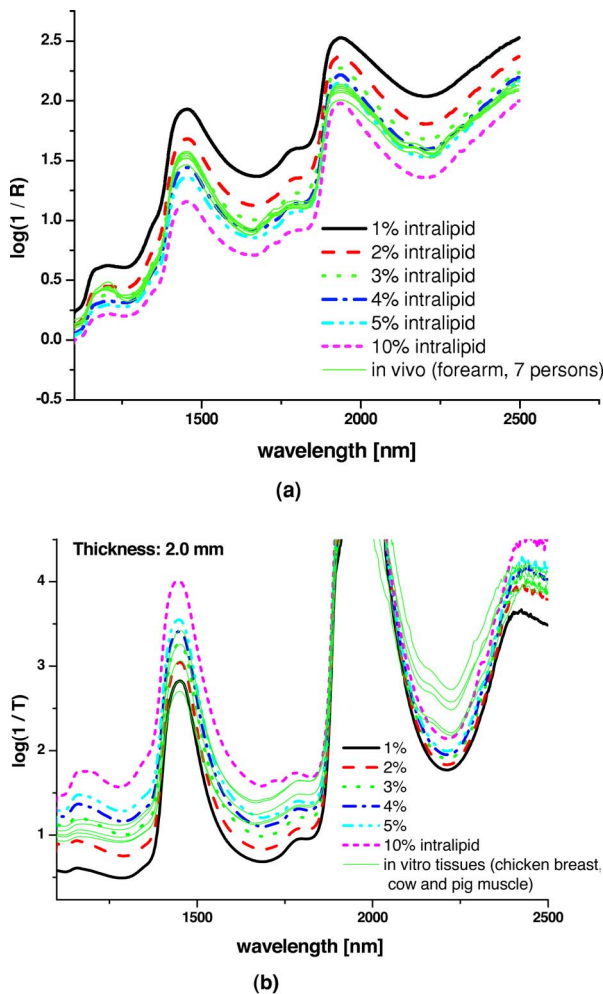
Fig. 2 Comparison between biological tissues and intralipid solutions: (a) reflectance from human forearm and the solutions of different intralipid concentration and (b) transmittance of biological tissues and intralipid solutions.
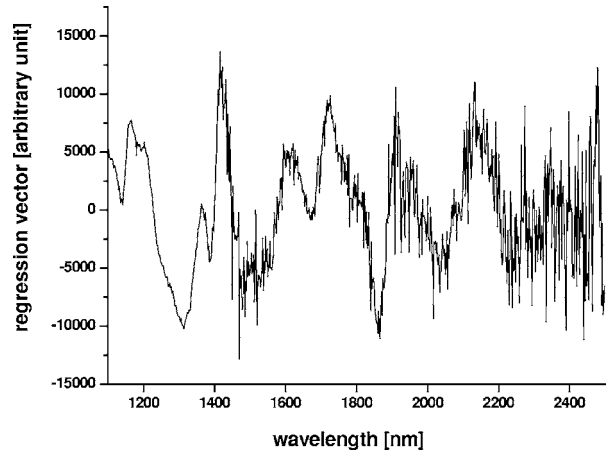
Fig. 3 Analysis of diffuse reflectance measurement in terms of the regression vector of the calibration model between 1100 and 2500 nm.

light illumination and detection, and there have been studies comparing different parts of the human body as measurement sites.[6,7]

Diffuse reflectance spectroscopy has been used widely in research and in attempts to commercialize noninvasive glucose monitoring.[8–11] In this paper, we investigate glucose prediction using reflectance and transmittance measurement set-ups. We prepared tissue phantoms that had scattering coefficients comparable to those of biological tissue. Small changes in the scattering of the samples were introduced to study the influence of scattering. Measurements were made between 1100 and 2500 nm, which includes both the overtone and combination absorption bands of glucose. Analysis was performed using PLSR.

2 Materials and Methods

To simulate biological tissue scattering, we chose intralipid as scatterers. Spectra were measured with a Foss™ NIR 6500 system between 1100 and 2500 nm with 2-nm steps (Fig. 1). The light source was a tungsten halogen lamp, and a PbS detector was used. The active area of detector was 1×1 cm^2. One detector was used for transmittance measurement and four detectors were employed for reflectance measurement. One scan time was 1 s and the 32 scan data were averaged to produce a spectrum. The system SNR of the measured spectrum was 10^{-5} absorbance, which was computed from two consecutively acquired spectra. We measured reflectance and transmittance of biological tissues and intralipid solutions to select a proper concentration of intralipid (Fig. 2).

Figure 2(a) shows reflectance measurements from 1 to 10% intralipid samples. We acquired diffuse reflectance from a 10-mm-thick cell for convenience, since reflectance spectra did not change for samples thicker than 2 mm. Figure 2(a) also contains reflectance spectra of the human body measured on the inner forearm. We put cosmetic oil on the skin to minimize the surface roughness and to ensure a close contact without an air gap between the skin and the detector window. Cosmetic oil, which is transparent at 1100 to 2500 nm, produced spectra of high repeatability. Reflectance from the human forearm is similar to that of a 4% intralipid sample, as
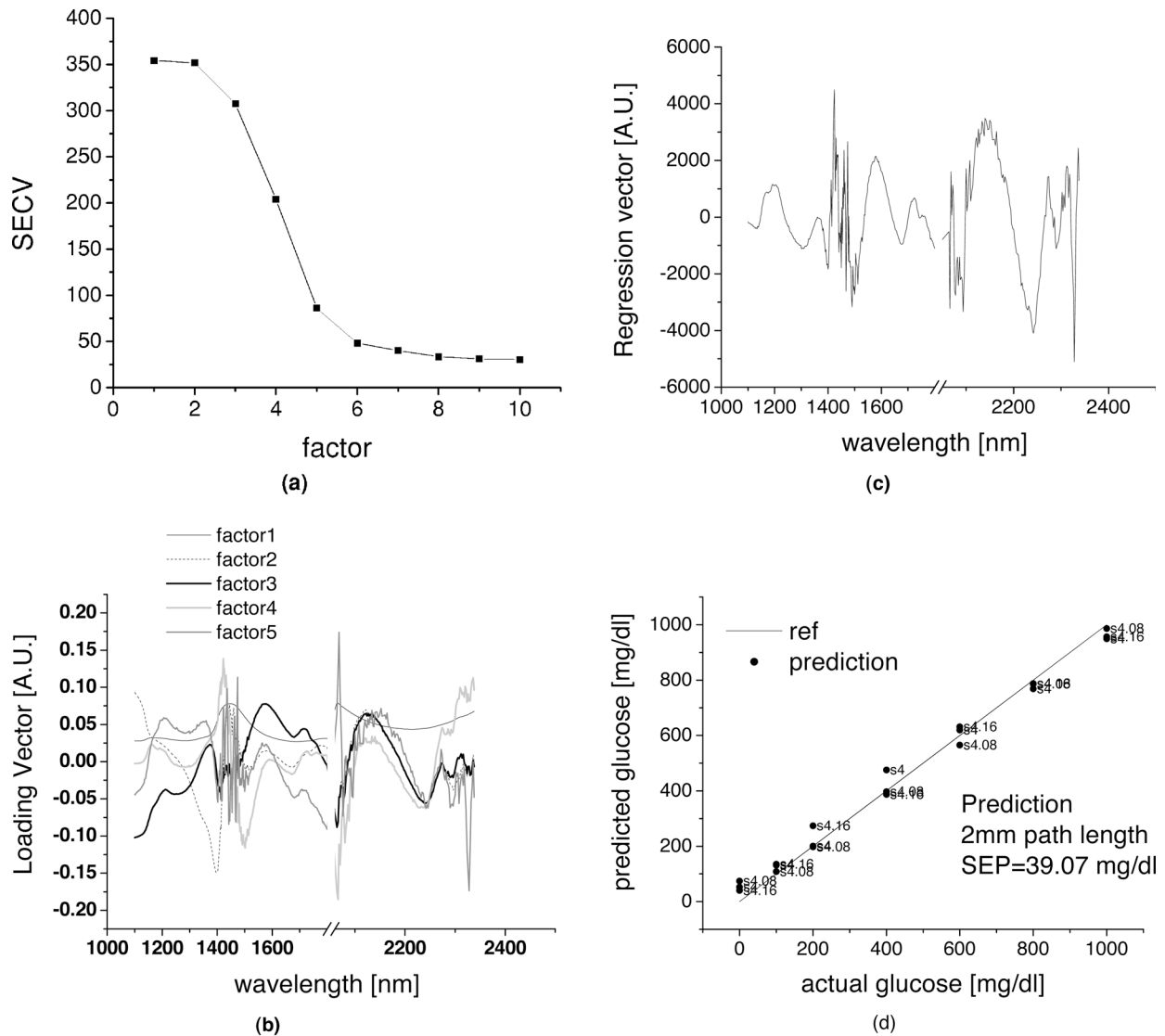
(a)

(c)

(b)

(d)

Fig. 4 Analysis for diffuse reflectance measurement between 1100 and 1850 nm: (a) SECV with respect to the optimal number of factor, (b) loading vector of calibration model, (c) regression vector of calibration model, and (d) prediction of glucose illustrated with the intralipid concentrations of sample solutions.

shown in Fig. 2(a). Figure 2(b) shows diffuse transmittance measurements from various samples. Intralipid samples had concentrations of 1 to 10%. Tissue samples were chicken breast, cow muscle, and pig muscle. The sample thickness was set to 2 mm for transmittance measurement. A solution of 4% intralipid was similar to biological tissue even though there were some differences at the combination band due to protein absorption. We chose 4% intralipid solutions as a tissue phantom.

Biological tissue is inhomogeneous and shows variations of scattering coefficients, depending on the samples. Therefore, we prepared samples with slight variations of intralipid concentrations to simulate tissue scattering variations. A 1.1% decrease of scattering coefficient was induced[12] by an increase of 1000 mg/dl glucose concentration at 1000 nm. Intralipid concentrations of 4, 4.08, and 4.16% were used as sample media. Seven levels of glucose concentrations ranging from

Fig. 5 Prediction results of reflectance measurement with the offset of medium scattering corrected.

Table 1 Calibration and prediction models in predicting glucose compared for the reflectance and transmittance methods.

	Wavelength Region (nm)	Calibration				Prediction		
		SECV (mg/dl)	R_{val}	SEC (mg/dl)	Number of Factor	SEP (mg/dl)	R_{pred}	Slope
Diffuse reflectance (10-mm-thick sample)	1100–2500	69.58	0.98	27.38	9	275.44	0.80	0.74
	1100–1850	33.51	1.00	15.91	8	437.54	0.98	0.89
	1850–2500	108.04	0.95	30.57	8	192.00	0.88	0.69
Diffuse transmittance (1-mm-thick sample)	1100–1800 2064–2338	38.29	0.99	3.22	9	24.69	1.00	1.01
	1100–1800	33.99	1.00	2.88	7	26.77	1.00	1.01
	2064–2338	13.90	1.00	4.50	8	43.51	1.00	1.03
Diffuse transmittance (2-mm-thick sample)	1100–1830 2050–2392	54.67	0.99	26.46	7	39.07	1.00	0.92
	1100–1830	62.73	0.98	40.47	7	83.58	0.99	0.95
	2050–2392	74.54	0.98	27.39	8	94.76	0.97	0.88
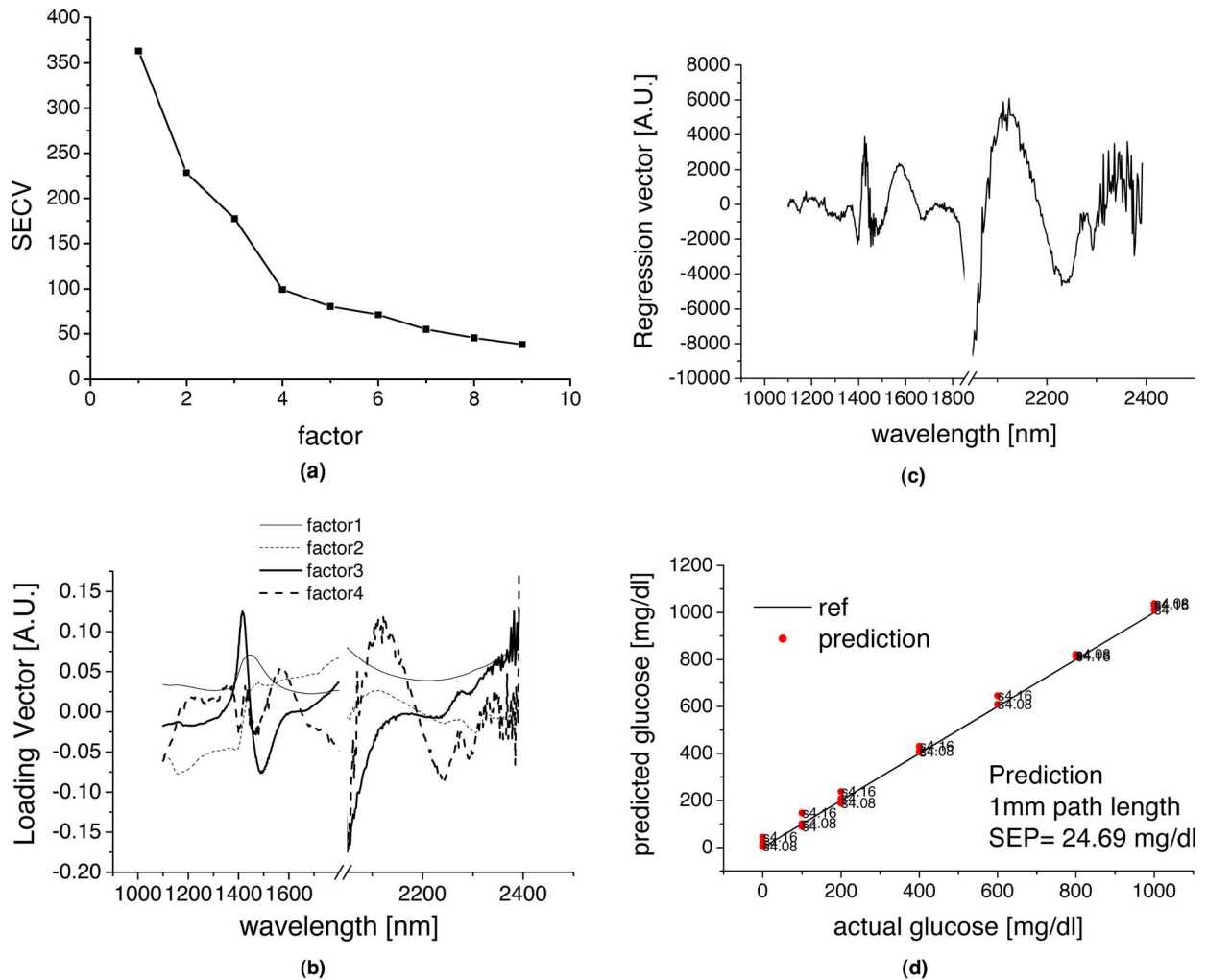
Fig. 6 Analysis for diffuse transmittance with 1-mm-thick samples: (a) SECV with respect to the optimal number of factor, (b) loading vector of calibration model, (c) regression vector of calibration model, and (d) prediction of glucose concentrations.

Fig. 7 Analysis for diffuse transmittance with 2-mm-thick samples: (a) SECV with respect to the optimal number of factor, (b) loading vector of calibration model, (c) regression vector of calibration model, and (d) prediction of glucose concentrations.

0 to 1000 mg/dl were prepared. Three samples were made for each glucose concentration to include the effect of sample-to-sample variations. A total 63 samples were prepared (7 glucose levels ×3 intralipid concentrations ×3 sample per each condition). The sample temperature was controlled at 30°C. We measured the spectrum of each sample in random order. Chemometric analysis was carried out using a Pirouette™ 3.0 (Infometrix, Woodinville, Washington, U.S.A).

3 Results and Discussion

Measured NIR spectra include information of not only glucose but also other components and are also affected by other phenomena such as scattering and system noise. A key objective of statistical analysis is to decrease the prediction error by minimizing spectral variation caused by anything other than glucose. Measured raw spectra were preprocessed for this purpose before the PLSR analysis. We used the multiplicative scatter correction (MSC) as data preprocessing to correct for

medium scattering. MSC assumes that the original signal can be recovered by the elimination of additive noise and multiplicative noise. The parameters are extracted from a linear regression of the ideal spectrum, and the original spectrum is reconstructed. The ideal spectrum is often simply the mean of the included spectra. We used the average spectra as the ideal MSC spectrum. Defining the mean spectrum as the ideal is sometimes regarded as a disadvantage of MSC. Although MSC may not be perfect in correcting multiple scattering, it is regarded as a better choice than other preprocessing methods.

The calibration model was constructed using PLSR models. For quantitative analysis of NIR spectra, full-frequency-range spectra are often used in conjunction with PLSR or principal component regression (PCR). NIR spectroscopy does not show individual vibration absorption since overlapping of absorption peaks of components results in relatively broad absorption bands. PLSR uses the concentration information during the decomposition process. This results in spec-

tra containing higher constituent concentrations that are more weighted than those with low concentrations. Thus, the eigenvectors and scores computed from PLSR analysis are different from those of PCR. The loading vectors of PLSR are directly related to the constituents of interest. Therefore, we used the loading vector to correlate with glucose information.

To choose optimal wavelength bands, we avoided the regions of high noise-to-signal ratio bands and water absorption bands, including the 1440- and 1940-nm regions. We compared accuracies at three wavelength regions. They were the overtone (1100 to 1850 nm) and combination (2050 to 2392 nm) bands of glucose and the entire region of 1100 to 2500 nm. The overtone band contains an absorption peak at 1688 nm originated 2υ of —CH, and the combination band has absorption peaks at 2261 and 2326 nm that are the combinations of a CH stretch and a CCH, OCH deformation, respectively.[13]

The calibration and prediction results were analyzed in terms of the standard error of cross validation (SECV), standard error of calibration (SEC), standard error of prediction (SEP), and regression coefficient of prediction (R_{pred}). On day 1, 21 samples of 7 glucose levels and 3 intralipid concentrations were made and their reflectance and transmittance spectra were measured. After 1 week from the first experiment, another 21 samples were made and their spectra were measured. After 2 weeks, the same procedure was repeated again. By doing this, the influences of day-to-day variations of spectral measurement as well as sample-to-sample variations were included. A total of 63 data were obtained for either reflectance or transmittance measurements. Two thirds of the total data were used as a calibration set and the remaining 21 data were used as a prediction set.

Table 1 summarizes the calibration and prediction results. Obviously SECs, compared with SECVs and SEPs, were the smallest with values between 3 and 40 mg/dl, depending on the wavelength regions. SECs were comparable to each other for the reflectance and transmittance with a 2-mm-thick sample. As expected, SECVs were longer than SECs, and SEPs were the largest. It is also obvious that SEPs should be used in discussing prediction accuracy rather than SECs or SECVs.

3.1 Diffuse Reflectance

For reflectance, SECV at the overtone band of 1100 to 1850 nm was better than other bands, and SEPs (437.5 mg/dl) were very large, but the regression coefficient (0.89) was acceptable (Table 1). SECs and SECVs were poorer at the combination band, which was unexpected since glucose absorption is much stronger at the combination band than at the overtone band. This was verified by regression vector analysis. Figure 3 shows regression vectors between 1100 and 2500 nm. Regression vectors were very noisy between 2200 and 2500 nm, which contains the combination band. Overall, the SEPs for reflectance measurement were too large to be used. Noisy regression spectral regions should be excluded for the stability of the calibration model.[14] This indicates that the calibration model does not contain reliable glucose absorption information. The result of calibration and prediction was the best in the overtone band (Table 1), so our
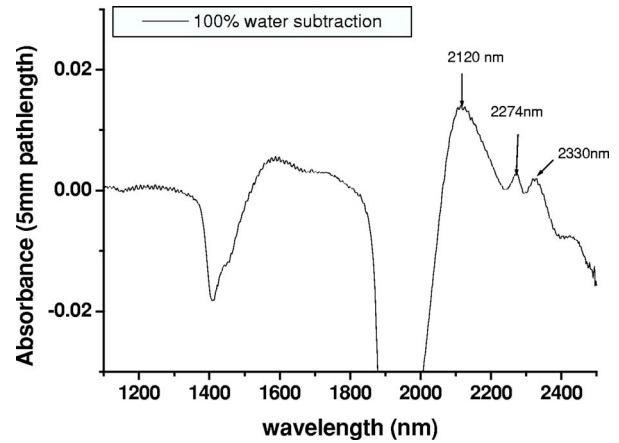

Fig. 8 Water-subtracted glucose spectrum. The glucose concentration is 5 g/dl.

study was focused on the overtone band in the reflection setup.

Further analysis on reflectance measurement in the overtone band was performed and the results are illustrated in Fig. 4. The optimal number of factors was eight from the F test, as in Fig. 4(a). The first loading vector shown as factor 1 in Fig. 4(b) was similar to a profile of the intralipid spectra. The regression vector of the calibration model is given in Fig. 4(c) and did not represent glucose absorption shape. The regression spectrum was very noisy in the overtone region. It appears that reflected light does not contain enough information on glucose absorption since the major portion of detected light is contributed by superficial layers. The mean path length of diffuse reflected light in the overtone region is as short as 0.25 mm when it is calculated with optical properties[15,16] of $\mu_a = 5.75$ cm^{-1} and $\mu_s' = 8.31$ cm^{-1}.

In addition, scattering changes due to not only glucose concentrations but also medium scattering might be influential factors in the reflectance regression model. This was proved by the observations in Fig. 4(d) that the calibration model gave the predicted values dependent on intralipid concentrations. In fact, SECVs and SEPs were very large for our case of reflectance measurement. Samples having different scattering backgrounds of 4, 4.08, and 4.16% intralipid concentrations might have contributed seemingly large values of SECVs and SEPs.

The prediction results are shown in Fig. 4(d). Large offset values appeared between the predicted values (in the dots) and reference values (in the line). The offset increased as the intralipid concentration increased from 4 to 4.16%. This indicates that the calibration model can have offsets induced by medium scattering and possibly by water displacement in the cell experiment. For an in vivo experiment, each measurement site has a different degree of scattering that may cause an offset in the predicted value. When the offset of each medium scattering was corrected by subtracting the predicted glucose concentration at 0 mg/dl of each scattering background, the prediction error was improved significantly, as given in Fig. 5. The SEP was 438 mg/dl and the offset-corrected SEP could be reduced to 61.4 mg/dl with a mean absolute error (MAE) of 13.9%.

3.2 Diffuse Transmittance

For the case of transmittance, using the entire spectrum of 1100 to 2400 nm produced the smallest errors (Table 1). Figures 6 and 7 display the results of transmittance measurements for 1- and 2-mm-thick samples, respectively. SECVs and SEPs for 1 mm thick sample were better than those for 2 mm sample. It appears to be related with the system S/N. Light penetration especially at the combination band is short. When a sample is thicker, light travels more and interacts more with the medium. However, the signal becomes weaker. Only about $0.1 \sim 1\%$ of light passes through a 2-mm sample at the combination band [see Fig. 2(b)]. The first loading vector noted as factor 1 had usually a mean-centered profile of sample spectrum. Higher order loading vectors (for example factor 4 in Fig. 6(b) and factor 3 in Fig. 7(b)) were similar to absorption spectra of water-subtracted glucose solution. Water-subtracted glucose spectrum is shown in Fig. 8. In Fig. 6(b) and Fig. 7(b), glucose peaks at the regions of 2120 nm, 2274 nm, and 2330 nm could be observed. The regression vectors showed that there was glucose absorption information as you can see in Fig. 6(c) and Fig. 7(c). The prediction results gave less offset or a dependency on the scatterers' concentration as depicted in Fig. 6(d) and Fig. 7(d).

4 Summary and Conclusion

We examined whether there was indeed glucose-related absorption information in the NIR spectroscopic method. Two different setups of reflectance and transmittance measurements were investigated. Intralipid solutions were used to simulate tissue scattering. We introduced the variations of scattering concentrations in the medium so that the influence of scattering background was studied during the prediction of glucose concentrations. Transmittance proved to be better than reflectance in terms of SECs and SEPs. Loading vectors and regression vectors calculated during PLSR models had spectral profiles of glucose-related information in the transmittance measurement. For the reflectance measurement, it was difficult to find glucose-related spectral profiles in the loading and regression vectors. For transmittance for all SEPs, SECVs, and SEPs, the thinner the sample thickness, the better were the results. From our investigation, we suggest that the transmittance setup is preferred for glucose monitoring.

References

1. M. R. Robinson, R. P. Eaton, D. M. Haaland, G. W. Keep, E. V. Thomas, B. R. Stalled, and P. L. Robinson, "Non-invasive glucose monitoring in diabetic patients: a preliminary evaluation," *Clin. Chem.* **38**, 1618–1622 (1992).
2. Y.-J. Kim and G. Yoon, "Multi-component assay for human serum using mid-infrared transmission spectroscopy based on component-optimized spectral region selected by first loading vector analysis," *Appl. Spectrosc.* **56**(5), 625–632 (2002).
3. Y.-J. Kim, S. Hahn, and G. Yoon, "Determination of glucose in whole blood samples by mid-infrared spectroscopy," *Appl. Opt.* **42**(4), 745–749 (2003).
4. L. Heinemann and G. Schmelzeisen, "Non-invasive continuous glucose monitoring in type I diabetic patients with optical glucose sensors," *Diabetologia* **41**, 848–854 (1998).
5. G. Kumar and J. M. Schmitt, "Optical probe geometry for near-infrared spectroscopy of biological tissue," *Appl. Opt.* **36**(10), 2286–2293 (1997).
6. J. J. Burmeister and M. A. Arnold, "Evaluating of measurement sites for noninvasive blood glucose sensing with near-infrared transmission spectroscopy," *Clin. Chem.* **45**, 1621–1627 (1999).
7. J. J. Burmeister, M. A. Arnold, and G. W. Small, "Non-invasive blood glucose measurements by near-infrared transmission spectroscopy across human tongue," *Diabetes Technol. Ther.* **2**, 5–16 (2000).
8. H. M. Heise, R. Marbach, T. Koschinsky, and F. A. Gries, "Noninvasive blood glucose sensors based on near-infrared spectroscopy," *Artif. Organs* **18**, 439–447 (1994).
9. S. F. Malin, T. L. Ruchti, T. B. Blank, S. N. Thennadil, and S. L. Monfre, "Noninvasive prediction of glucose by near-infrared diffuse reflectance spectroscopy," *Clin. Chem.* **45**(9), 1651–1658 (1999).
10. T. B. Blank, T. L. Ruchti, A. D. Lorenz, S. L. Monfre, M. R. Makarewicz, M. Mattu, and K. H. Hazen, "Clinical result from a non-invasive blood glucose monitor," *Proc. SPIE* **4624**, 1–10 (2002).
11. P. J. Cooper and T. Q. Barker, "Individual calibration of blood glucose for support noninvasive self-monitoring blood glucose," U.S. Patent No. 6,309,884 (2001).
12. M. Kohl and M. Cope, "Influence of glucose concentration on light scattering in tissue-simulating phantom," *Opt. Lett.* **19**, 2170–2172 (1994).
13. O. S. Khalil, "Spectroscopic and clinical aspects of noninvasive glucose measurements," *Clin. Chem.* **45**, 165–177 (1999).
14. J. M. Brenchley, U. W. E. Horchner, and J. H. Kalivas, "Wavelength selection characterization for NIR spectra," *Appl. Spectrosc.* **51**, 689–699 (1997).
15. T. L. Troy and S. N. Thennadil, "Optical properties of human skin in the near infrared wavelength range of 1000 to 2200 nm," *J. Biomed. Opt.* **6**, 167–176 (2001).
16. M. S. Patterson, B. Chance, and B. C. Wilson, "Time resolved reflectance and transmittance for the non-invasive measurement of tissue optical properties," *Appl. Opt.* **28**, 2331–2335 (1989).